Chemosensors

DOI: 10.1002/anie.201406585

Chiroptical Detection of Nonchromophoric, Achiral Guests by Enantiopure Alleno-Acetylenic Helicages**

*Ori Gidron, Marc-Olivier Ebert, Nils Trapp, and François Diederich**

In memory of Michael Bendikov

Abstract: *Enantiopure alleno-acetylenic ligands assemble diastereoselectively upon the addition of a zinc(II) salt to form triple-stranded helicates, which provide a sufficiently large helical cage ("helicage") for the encapsulation of guests. The inclusion complexation of heteroalicycles is confirmed by ROESY and DOSY NMR spectroscopy and quantified in ^{1}H NMR binding titrations. The ECD spectra of the helicates, which showed strong Cotton effects and exciton coupling, were found to be extremely sensitive to the nature of the guest molecules. Consequently, a series of nonchromophoric, achiral guests of different sizes as well as regioisomers (1,3- and 1,4-dioxane) became distinguishable on the basis of their induced CD (ICD) spectra. Molecular dynamics (MD) simulations show the adaptability of the cavity size to individual guest molecules and support the selective ICD output. Particularly high affinity towards 1,4-dioxane allowed its selective detection at parts-per-million (ppm) levels in aqueous solutions.*

Supramolecular coordination chemistry enables the formation of complex structures—many of which are inspired by nature—and as such their function as guest-specific receptors is of major relevance.[1] Helicates are a particularly interesting class of supramolecular assemblies, widely investigated for their elegant and intrinsically chiral structure.[2,3] While the enantioselective interaction of helicates with large biological molecules, such as DNA and proteins, has been extensively studied,[4] examples of their function as receptors which can encapsulate small organic guests are rare.[5] In such systems, the prospect of detecting chiroptical changes induced by external stimuli is attractive, mainly because of potential applications in chemosensors due to the simplicity of the method and low detection limits.[6] While most examples of chiroptical sensing require a chiral or chromophoric guest, the chiroptical sensing of achiral, nonchromophoric guests is more challenging.[6,7] For such a selective response the receptor must have strong chiroptical properties (e.g. strong Cotton effects) to allow the detection of small conformational changes upon guest complexation.

Recently, our group developed enantiomerically pure 1,3-diethynylallene **1**[8] (Scheme 1) as an optically and thermally stable building block for the construction of alleno-acetylenic oligomers[9] and macrocycles,[10] which displayed outstanding chiroptical properties. Rigidification of the backbones resulted in further enhancement of these properties.[11] We therefore became interested in transferring the molecular properties of alleno-acetylenes to supramolecular assemblies.

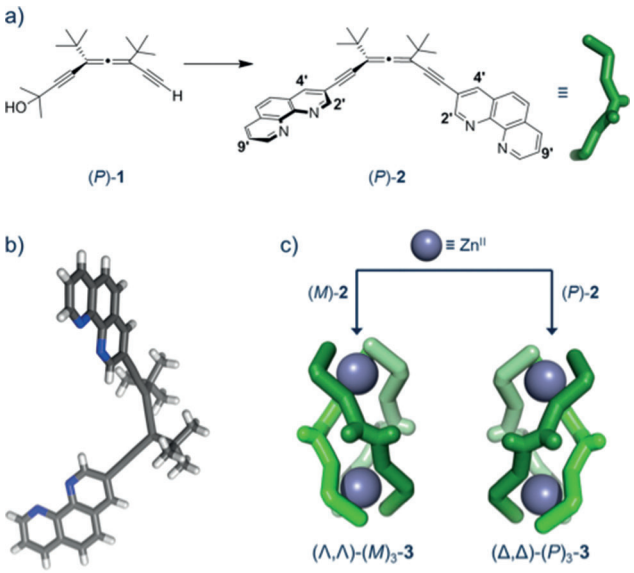

Scheme 1. a) Synthesis of (*P*)-**2**; reagents and conditions: 1. 3-Bromophenanthroline, K_3PO_4, $[Pd(MeCN)_2Cl_2]$ (5 mol%), XPhos (10 mol%), (*P*)-**1**, Me_2SO, 85 °C, 12 h. 2. Tetrabutylammonium hydroxide (40 wt% in methanol, 10 mol%), 12 h. b) Crystal structure of (*P*)-**2** (space group *C*2, solvent molecules omitted for clarity). c) Assembly of helicates (Λ,Λ)-(*M*)$_3$-**3** and (Δ,Δ)-(*P*)$_3$-**3**. XPhos = 2-Dicyclohexylphosphino-2′,4′,6′-triisopropylbiphenyl.

Herein, we describe the diastereoselective assembly of alleno-acetylenes (*M*)-**2** and (*P*)-**2** to form triple-stranded helicates (Λ,Λ)-(*M*)$_3$-**3** and (Δ,Δ)-(*P*)$_3$-**3**, respectively (Scheme 1), with the lean all-carbon backbones of the alleno-acetylene moieties forming enantiopure helical cages ("helicages"). The X-ray structure of (Λ,Λ)-(*M*)$_3$-**3** revealed an internal cavity for the encapsulation of guests, as observed

[*] Dr. O. Gidron, Dr. M.-O. Ebert, Dr. N. Trapp, Prof. Dr. F. Diederich
Laboratorium für Organische Chemie, ETH Zürich
Vladimir-Prelog-Weg 3, CH-8093 Zurich (Switzerland)
E-mail: diederich@org.chem.ethz.ch

[**] This work was supported by the ERC Advanced Grant No. 246637 ("OPTELOMAC"). O.G. acknowledges a Marie-Curie fellowship from the European Union Seventh Framework Programme (FP7/2007–2013) under grant agreement no. 327582. We are grateful to Michael Solar for his help in recording the X-ray diffractograms. We thank Dr. Bruno Bernet and Dr. David Schweinfurth for their useful comments. X-ray services were provided by the Small Molecule Crystallography Center of ETH Zürich (http://www.smocc.ethz.ch).

Supporting information for this article is available on the WWW under http://dx.doi.org/10.1002/anie.201406585.

by ROESY and DOSY NMR experiments. The ECD (electronic circular dichroism) spectra of (Λ,Λ)-$(M)_3$-**3** and (Δ,Δ)-$(P)_3$-**3** were found to be extremely sensitive to the nature of the guest molecules, allowing the selective detection of nonchromophoric, achiral guests. Particularly high affinity towards 1,4-dioxane enabled its selective detection at ppm (parts per million) levels.

Ligands (*M*)-**2** and (*P*)-**2** were prepared in a one-pot procedure from (*M*)-**1** and (*P*)-**1**, respectively.[8] Copper-free Sonogashira coupling[12b,c] with 3-bromophenanthroline,[12a] followed by subsequent removal of the acetonide group with a catalytic amount of tetrabutylammonium hydroxide,[12d] allowed the second Sonogashira coupling to proceed, with an overall yield of 35% (Scheme 1a). Phenanthroline (phen) was chosen for its synthetic variability, allowing future construction of heteroleptic supramolecular assemblies.[13]

Mixing enantiopure (*P*)-**2** with $Zn(OTf)_2$ in a ratio of 3:2 resulted in the immediate formation of (Δ,Δ)-$(P)_3$-**3** (Scheme 1c). The high-resolution electrospray-ionization mass spectrum (HR-ESI-MS) of (Δ,Δ)-$(P)_3$-**3** revealed signals of the differently charged species $\{Zn_2[(P)\text{-}\mathbf{2}]_3(OTf)_2\}^{2+}$, $\{Zn_2[(P)\text{-}\mathbf{2}]_3(OTf)\}^{3+}$, and $\{Zn_2[(P)\text{-}\mathbf{2}]_3\}^{4+}$ ($m/z = 1049.3$, 649.5, and 449.9, respectively, Figure S9 in the Supporting Information). The ^{1}H NMR spectrum of (Δ,Δ)-$(P)_3$-**3** displayed only seven aromatic signals, corresponding to the formation of a single species and excluding the formation of a nonsymmetrical "mesocate" (nonhelical conformer with the two metal centers in the Δ,Λ conformation).[3] In addition, ROESY NMR experiments showed a strong correlation between the *tert*-butyl protons ($C(CH_3)_3$) and H-4′ and H-2′, with the cross-peak for H-4′ being significantly more intensive than that for H-2′ (Figure S8). This confirms that the bis-phenanthroline ligand adopts the same conformation in the assembly as that observed for the free state, which should result in right-handed helicates for (*P*)-**2** ligands and left-handed helicates for (*M*)-**2** ligands consisting of (Δ,Δ) and (Λ,Λ) metal centers, respectively (Scheme 1c). Assembly of a solution of racemic (*M*/*P*)-**2** with $Zn(OTf)_2$ resulted in narcissistic self-sorting to form exclusively helicates (Λ,Λ)-$(M)_3$-**3** and (Δ,Δ)-$(P)_3$-**3** as confirmed by the fact that their NMR spectra were identical to those obtained starting from enantiopure (*M*)- or (*P*)-**2**.[14]

The structure of (Λ,Λ)-$(M)_3$-**3** was further substantiated by X-ray analysis of single crystals, which were obtained by slow diffusion of diethyl ether in an acetonitrile solution and contained $Zn_2[(M)\text{-}\mathbf{2}]_3(ClO_4)_4$ in the *P*1 triclinic space group (Figure 1). The triple-stranded helicate features an internal cavity occupied by two acetonitrile molecules, antiparallel to each other.[15] As a result, the complex is distorted from C_3 to C_1 symmetry, with two strands "opening" to better accommodate the second acetonitrile molecule, as can be observed in the different views shown in Figure 1.[16] Importantly, changes in the orientation of alleno-acetylenic chromophores around the metal centers should induce significant changes in the ECD spectra due to the expected exciton coupling.[6c,17]

Based on the above-mentioned X-ray structure, we expected the encapsulation of guests within the cavity to proceed also in solution. Indeed, the addition of small cyclic guests in methanol resulted in upfield chemical shifts at saturation binding ($-\Delta\delta_{sat}$) of up to 0.28 ppm for protons H-2′ and H-9′, as observed by ^{1}H NMR spectroscopy. This can be attributed to conformational changes in the helicate upon guest complexation. ROESY NMR spectra shows correlation between the guest molecule (1,4-dioxane) and H-2′ in the host (Figure 2a), while no correlation is observed between the host and the solvent (CD_3OD). DOSY NMR spectra[18] of 1,4-dioxane⊂(Λ,Λ)-$(M)_3$-**3** revealed that the diffusion value for the encapsulated guest is between that of the free 1,4-dioxane and that of helicate (Λ,Λ)-$(M)_3$-**3**, an indication of a fast guest exchange on the DOSY timescale (Figure 2b).

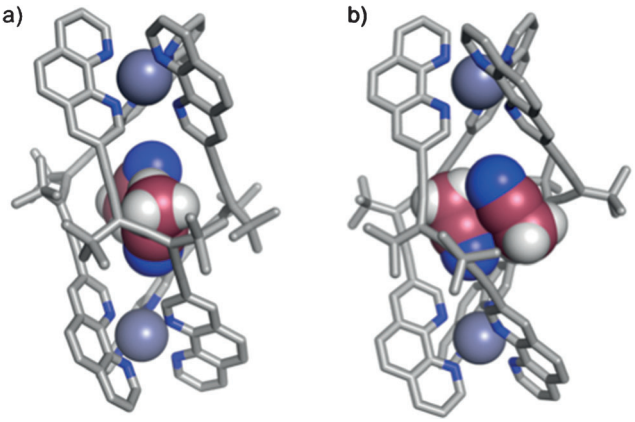

Figure 1. Two views of the crystal structure of helicate (Λ,Λ)-$(M)_3$-**3** (*P*1 space group) with two encapsulated, antiparallel acetonitrile molecules. Anions, additional outside solvent molecules, and hydrogen atoms are omitted for clarity.[15]

Importantly, the diffusion rate of (Λ,Λ)-$(M)_3$-**3** does not change upon addition of 1,4-dioxane, which indicates that (Λ,Λ)-$(M)_3$-**3** most likely retains its triple-helicate configuration upon guest complexation. This is in contrast to other helicates, which upon introduction of guests transform to larger tetrahedral structures to enable complexation (for additional DOSY and ROESY experiments, see Sections S4.3 and S4.4 in the Supporting Information).[19]

The binding constants for various alicyclic and heteroalicyclic guests were obtained by nonlinear least-squares fitting of ^{1}H NMR titration data at fast exchange, with constant host and varying guest concentration. A 1:1 binding stoichiometry was inferred from Job plot analysis (Figure S34). With CD_3OD as the solvent, most guests displayed weak binding constants ($K_a = 11$–$35\,M^{-1}$, see Table 1; for titration curves, see Section S4.1). The ideal guest size seems to be five- and six-membered rings, while the larger cycloheptane as well as aromatic rings (pyrazine, *p*-xylene, and furan) show no binding. While the presence of one oxygen atom in tetrahydropyran only slightly improves the binding affinity ($K_a = 35\,M^{-1}$) in CD_3OD relatve to that of cyclohexane ($K_a = 24\,M^{-1}$), 1,4-dioxane shows significantly stronger binding ($K = 570\,M^{-1}$). In addition, unlike other guests, which show almost no change in their ^{1}H NMR signals upon encapsulation, the 1,4-dioxane singlet is split upon encapsulation, since its protons become diastereotopic inside the enantiopure host (Figure 2c). In sharp contrast, regioisomeric 1,3-dioxane only binds weakly ($K_a = 11\,M^{-1}$).

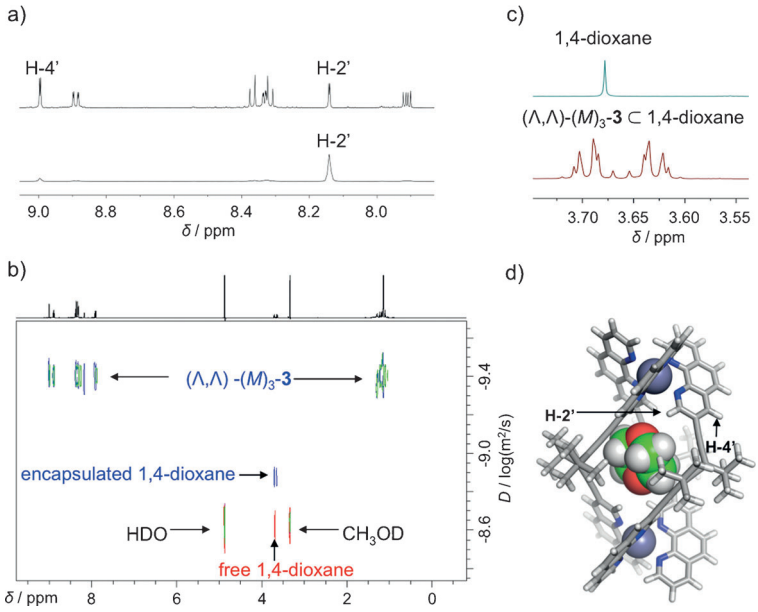

Figure 2. a) ^{1}H NMR spectrum of 1,4-dioxane⊂(Λ,Λ)-$(M)_3$-**3** (top) and 1D trace of the ROESY NMR spectrum at 3.65 ppm, showing correlation between 1,4-dioxane and H-2′ located inside the cavity of (Λ,Λ)-$(M)_3$-**3**. b) Overlay of DOSY NMR traces, top: free (green) (Λ,Λ)-$(M)_3$-**3** and 1,4-dioxane⊂(Λ,Λ)-$(M)_3$-**3** (blue); middle: bound 1,4-dioxane (blue); bottom: free 1,4-dioxane (red) and solvent (all three colors). (c) ^{1}H NMR spectra of free 1,4-dioxane and in 1,4-dioxane⊂(Λ,Λ)-$(M)_3$-**3**. d) Calculated structure (DFT/B3LYP/6-31G(d)) of 1,4-dioxane⊂(Δ,Δ)-$(P)_3$-**3**. All NMR spectra measured in CD_3OD at 298 K.

Table 1: Binding parameters at 298 K for the complexation of various guests by (Λ,Λ)-$(M)_3$-**3** in CD_3OD.

Guest	CD_3OD		D_2O/CD_3OD 1:1	
	K_a [M^{-1}][a]	$-\Delta\delta_{sat}$(H-2′) [ppm][b]	K_a [M^{-1}][a]	$-\Delta\delta_{sat}$(H-2′) [ppm][b]
1,3-dioxane	11	0.20	30	0.18
1,4-dioxane[c]	570	0.17	1800	0.10
tetrahydrofuran	34	0.16	110	0.15
oxetane	13	0.28	30	0.28
cyclopentane	28	0.24	2200	0.21
tetrahydropyran	35	0.19	220	0.14
cyclohexane	24	0.22	1730	0.24
thiane	120	0.16	860	0.18
oxepane	11	0.12	[d]	[d]
(*R*)-(+)-1,2-epoxybutane	14	0.13	31	0.18
(*S*)-(−)-1,2-epoxybutane	16	0.14	49	0.21

[a] The association constant K_a was determined by nonlinear least-squares curve fitting of the ^{1}H NMR chemical shift of proton H-2′ located inside the cavity of (Λ,Λ)-$(M)_3$-**3**, assuming a 1:1 isotherm. Host (Λ,Λ)-$(M)_3$-**3** was titrated with guest, keeping the concentration of (Λ,Λ)-$(M)_3$-**3** constant (see Section S4.1 for details). Error estimated in the range of ±20%. [b] Calculated change in chemical shift at saturation binding, $-\Delta\delta_{sat}$. The − sign indicates an upfield shift. [c] 1,4-Dioxane binds in CD_3CN with $K_a = 9\,M^{-1}$ ($-\Delta\delta_{sat}$(H-2′) 0.17 ppm). [d] The chemical shift change was too small to be evaluated.

We performed solvent-dependent binding studies and expectedly found very weak complexation for 1,4-dioxane in acetonitrile ($K_a = 9\,M^{-1}$), which acts as a competitive inhibitor as suggested by the X-ray crystallographic findings (Figure 1). Increasing the solvent polarity (D_2O/CD_3OD 1:1) resulted in an increase in binding affinity. A particularly significant increase by 2 orders of magnitude was observed for hydrophobic cyclohexane and cyclopentane, reaching K_a values of $2\times10^3\,M^{-1}$. The large difference in binding affinity between 1,4- and 1,3-dioxane was also observed in the aqueous solutions, with K_a values of 1800 (1,4) versus $30\,M^{-1}$ (1,3) in D_2O/CD_3OD 1:1, and 8200 versus $860\,M^{-1}$ in H_2O/MeOH 19:1. The latter values were extracted from ECD titrations due to limited solubility of the host (see Section S4.1).

The strong binding of 1,4-dioxane is explained by the calculated (DFT/B3LYP/6-31G(d))[20] structure of 1,4-dioxane⊂(Δ,Δ)-$(M)_3$-**3**, which shows the two oxygen atoms facing toward the electropositive metal centers (Figure 2d), in a similar manner to the two N-nitrogen atoms of the antiparallel acetonitrile molecules observed in the X-ray structure (Figure 1). This notion is also supported by the increase in binding affinity upon replacement of oxygen with sulfur, exemplified for the binding of thiane compared with that of tetrahydropyran ($860\,M^{-1}$ versus $110\,M^{-1}$ in D_2O/CD_3OD 1:1), since the more diffuse sulfur is attracted strongly to the outer sphere of the metal centers.[21]

The ECD spectra of (Λ,Λ)-$(M)_3$-**3** and (Δ,Δ)-$(P)_3$-**3** in acetonitrile show strong exciton coupling with a large Cotton effect at 363 nm ($\Delta\varepsilon = 345\,M^{-1}cm^{-1}$), as expected for adjacent chromophores in octahedral alignment around the metal centers (Figure 3a).[17] Unlike the ECD spectra of alleno-acetylenes (*P*)-**1** and (*P*)-**2**, (as well as of other previously studied alleno-acetylenes), the spectra of (Δ,Δ)-$(P)_3$-**3** are sensitive to differences in temperature (see Section S5.3). The strong Cotton effect of the alleno-acetylene chromophores, combined with the high sensitivity of exciton coupling to the orientation of the chromophores, should result in a significant induced CD (ICD) upon guest complexation to the helicate.[6] Indeed, the addition of various guests to the helicate in methanol gave rise to strong ICD signals (up to $\Delta\Delta\varepsilon$ values of $70\,M^{-1}cm^{-1}$). The increase in Cotton effect upon guest encapsulation suggests a net effect of the guests on the helicate conformation. Importantly, the ICD spectra were found to be highly guest-dependent, where even regioisomers such as 1,4-dioxane and 1,3-dioxane produce clearly distinguishable spectra (Figure 3b). Variations in guest size also affect the ICD spectra as observed for the series of oxetane, tetrahydrofuran, and tetrahydropyran, most likely due to different conformational induction on the helicate (Figure 3c). Molecular dynamic (MD) simulations, followed by volume calculation using VOIDOO, determined the cavity size upon encapsulation of 1,4-dioxane and oxepane.[22] The difference in the average cavity size (135 Å^3 versus 154 Å^3 for 1,4-dioxane and oxepane, corresponding to a volume occupancy of 63% and 70%, respectively) confirms the dynamic nature of the helicage, which can adjust its size and shape based on the guest molecule ("induced fit").[23,24] This contributes to the sensitivity in the ICD output for different guests.

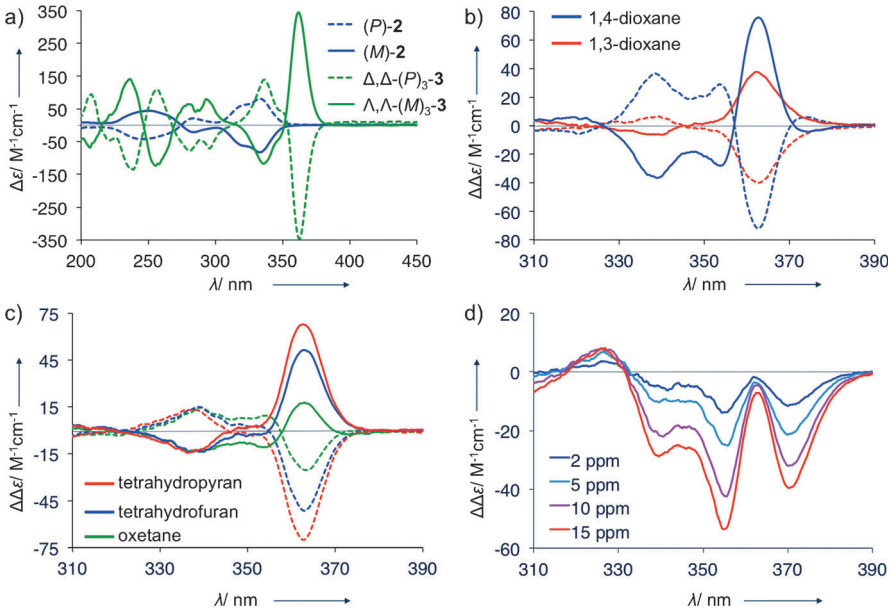

Figure 3. a) ECD spectra of (Λ,Λ)-$(M)_3$-**3** (green solid), (Δ,Δ)-$(P)_3$-**3** (green dashed), (*M*)-**2** (blue solid) and (*P*)-**2** (blue dashed) at 298 K in acetonitrile. b) ICD spectra of (Λ,Λ)-$(M)_3$-**3** (solid) and (Δ,Δ)-$(P)_3$-**3** (dashed) with 1% (v/v) 1,4-dioxane (blue) and 1,3-dioxane (red). (c) ICD spectra of (Λ,Λ)-$(M)_3$-**3** (solid) and (Δ,Δ)-$(P)_3$-**3** (dashed) with 1% (v/v) tetrahydropyran (red), tetrahydrofuran (blue), and oxetane (green). (d) ICD spectra of stepwise addition of 1,4-dioxane to (Λ,Λ)-$(M)_3$-**3** in H_2O/MeOH 19:1 at 295 K. Spectra shown in Figure 3 b,c were measured in methanol at 295 K. In Figure 3 b–d the spectrum of the free helicate was subtracted.

We were able to detect ppm levels of 1,4-dioxane in aqueous solutions containing 5% (v/v) of the helicate in MeOH, where at a level of 2 ppm of 1,4-dioxane the distinct peaks at 355 nm and 370 nm could be observed (Figure 3 d). In addition, 10 ppm of 1,4-dioxane, a class 2B carcinogen,[25] could be clearly detected even in the presence of 10 equivalents 1,3-dioxane, demonstrating the use of ICD as a sensitive method for the selective detection of achiral, nonchromophoric guests (Figure S43).

In summary, enantiopure alleno-acetylenes and Zn^{II} ions assemble diastereoselectively to form triple-stranded helicages, displaying strong chiroptical properties. They feature an interior cavity shaped by the lean alleno-acetylenic backbones, and various small cyclic guests form inclusion complexes with high selectivity. The intrinsically strong Cotton effect of alleno-acetylenes combined with exciton coupling allows for the chiroptical detection of nonchromophoric, achiral guests in a highly selective manner, as exemplified for the regioisomers 1,3- and 1,4-dioxane. MD simulations show the adaptability of the cavity size to individual guest molecules and support the selective ICD output. Particularly strong binding was observed for 1,4-dioxane, enabling its chiroptical detection in the low ppm concentration range. We are now extending the triple-helicates to systems containing multiple cavity binding sites and will investigate allosteric effects on guest recognition at these sites.

Received: June 25, 2014
Revised: September 24, 2014
Published online: November 10, 2014

Keywords: alleno-acetylenes · chiroptical chemosensors · host–guest complexation · supramolecular chemistry · triple helicates

[1] a) S. Sato, T. Murase, M. Fujita in *Supramolecular Chemistry: From Molecules to Nanomaterials, Vol. 5* (Eds.: P. A. Gale, J. W. Steed), Wiley, Chichester, **2012**, pp. 2071–2084; b) T. R. Cook, Y.-R. Zheng, P. J. Stang, *Chem. Rev.* **2013**, *113*, 734–777; c) T. K. Ronson, S. Zarra, S. P. Black, J. R. Nitschke, *Chem. Commun.* **2013**, *49*, 2476–2490.

[2] a) J. M. Lehn, A. Rigault, J. Siegel, J. Harrowfield, B. Chevrier, D. Moras, *Proc. Natl. Acad. Sci. USA* **1987**, *84*, 2565–2569; b) C. Piguet, G. Bernardinelli, B. Bocquet, A. Quattropani, A. F. Williams, *J. Am. Chem. Soc.* **1992**, *114*, 7440–7451; c) R. Krämer, J. M. Lehn, A. De Cian, J. Fischer, *Angew. Chem. Int. Ed. Engl.* **1993**, *32*, 703–706; *Angew. Chem.* **1993**, *105*, 764–767; d) G. Seeber, B. E. F. Tiedemann, K. N. Raymond, *Top. Curr. Chem.* **2006**, *265*, 147–183; e) R. M. Yeh, K. N. Raymond, *Inorg. Chem.* **2006**, *45*, 1130–1139; f) M. Berg, A. Lützen in *Metallofoldamers* (Eds.: G. Maayan, M. Albrecht), Wiley, Chichester, **2013**, pp. 125–158.

[3] J. Bunzen, T. Bruhn, G. Bringmann, A. Lützen, *J. Am. Chem. Soc.* **2009**, *131*, 3621–3630.

[4] a) I. Meistermann, V. Moreno, M. J. Prieto, E. Moldrheim, E. Sletten, S. Khalid, P. M. Rodger, J. C. Peberdy, C. J. Isaac, A. Rodger, M. J. Hannon, *Proc. Natl. Acad. Sci. USA* **2002**, *99*, 5069–5074; b) S. E. Howson, A. Bolhuis, V. Brabec, G. J. Clarkson, J. Malina, A. Rodger, P. Scott, *Nat. Chem.* **2012**, *4*, 31–36; c) H. Yu, M. Li, G. Liu, J. Geng, J. Wang, J. Ren, C. Zhao, X. Qu, *Chem. Sci.* **2012**, *3*, 3145–3153.

[5] a) T. Haino, H. Shio, R. Takano, Y. Fukazawa, *Chem. Commun.* **2009**, 2481–2483; b) W. Xuan, M. Zhang, Y. Liu, Z. Chen, Y. Cui, *J. Am. Chem. Soc.* **2012**, *134*, 6904–6907.

[6] a) G. A. Hembury, V. V. Borovkov, Y. Inoue, *Chem. Rev.* **2008**, *108*, 1–73; b) H. Miyake, H. Tsukube, *Chem. Soc. Rev.* **2012**, *41*, 6977–6991; c) C. Wolf, K. W. Bentley, *Chem. Soc. Rev.* **2013**, *42*, 5408–5424; d) G. Pescitelli, L. Di Bari, N. Berova, *Chem. Soc. Rev.* **2014**, *43*, 5211–5233.

[7] a) H. Maeda, Y. Bando, K. Shimomura, I. Yamada, M. Naito, K. Nobusawa, H. Tsumatori, T. Kawai, *J. Am. Chem. Soc.* **2011**, *133*, 9266–9269; b) J.-m. Suk, V. R. Naidu, X. Liu, M. S. Lah, K.-S. Jeong, *J. Am. Chem. Soc.* **2011**, *133*, 13938–13941; c) T. Ogoshi, D. Yamafuji, T. Akutsu, M. Naito, T.-a. Yamagishi, *Chem. Commun.* **2013**, *49*, 8782–8784.

[8] a) R. C. Livingston, L. R. Cox, V. Gramlich, F. Diederich, *Angew. Chem. Int. Ed.* **2001**, *40*, 2334–2337; *Angew. Chem.* **2001**, *113*, 2396–2399; b) R. Livingston, L. R. Cox, S. Odermatt, F. Diederich, *Helv. Chim. Acta* **2002**, *85*, 3052–3077; c) J. L. Alónso-Gomez, P. Schanen, P. Rivera-Fuentes, P. Seiler, F. Diederich, *Chem. Eur. J.* **2008**, *14*, 10564–10568.

[9] P. Rivera-Fuentes, J. L. Alónso-Gómez, A. G. Petrovic, F. Santoro, N. Harada, N. Berova, F. Diederich, *Angew. Chem.*

Int. Ed. **2010**, *49*, 2247 – 2250; *Angew. Chem.* **2010**, *122*, 2296 – 2300.

[10] a) J. L. Alonso-Gómez, P. Rivera-Fuentes, N. Harada, N. Berova, F. Diederich, *Angew. Chem. Int. Ed.* **2009**, *48*, 5545 – 5548; *Angew. Chem.* **2009**, *121*, 5653 – 5656; b) P. Rivera-Fuentes, J. L. Alónso-Gómez, A. G. Petrovic, P. Seiler, F. Santoro, N. Harada, N. Berova, H. S. Rzepa, F. Diederich, *Chem. Eur. J.* **2010**, *16*, 9796 – 9807.

[11] E. Donckele, O. Gidron, N. Trapp, F. Diederich, *Chem. Eur. J.* **2014**, *20*, 9558 – 9566.

[12] a) D. Tzalis, Y. Tor, S. Failla, J. S. Siegel, *Tetrahedron Lett.* **1995**, *36*, 3489 – 3490; b) D. Gelman, S. L. Buchwald, *Angew. Chem. Int. Ed.* **2003**, *42*, 5993 – 5996; *Angew. Chem.* **2003**, *115*, 6175 – 6178; c) E. Shirakawa, T. Kitabata, H. Otsuka, T. Tsuchimoto, *Tetrahedron* **2005**, *61*, 9878 – 9885; d) J. Li, P. Huang, *Beilstein J. Org. Chem.* **2011**, *7*, 426 – 431.

[13] a) G. Accorsi, A. Listorti, K. Yoosaf, N. Armaroli, *Chem. Soc. Rev.* **2009**, *38*, 1690 – 1700; b) K. Mahata, M. L. Saha, M. Schmittel, *J. Am. Chem. Soc.* **2010**, *132*, 15933 – 15935; c) J. Fan, M. L. Saha, B. Song, H. Schönherr, M. Schmittel, *J. Am. Chem. Soc.* **2012**, *134*, 150 – 153.

[14] a) M. A. Masood, E. J. Enemark, T. D. P. Stack, *Angew. Chem. Int. Ed.* **1998**, *37*, 928 – 932; *Angew. Chem.* **1998**, *110*, 973 – 977; b) C. Gütz, R. Hovorka, G. Schnakenburg, A. Lützen, *Chem. Eur. J.* **2013**, *19*, 10890 – 10894.

[15] It should be noted that the above-mentioned solvent model, consisting of two acetonitrile molecules inside the cavity in an antiparallel fashion applies for 75% of the structure, while in 25% of the structures the cavity is occupied by only one acetonitrile molecule, orthogonal to the Zn–Zn vector. See Section S6.3 for further discussion.

[16] D. L. Caulder, K. N. Raymond, *Acc. Chem. Res.* **1999**, *32*, 975 – 982.

[17] a) N. Harada, K. Nakanishi, *Circular Dichroic Spectroscopy—Exciton Coupling in Organic Stereochemistry*, Oxford University Press, Oxford, **1983**; b) G. Pescitelli, L. Di Bari, N. Berova, *Chem. Soc. Rev.* **2011**, *40*, 4603 – 4625; c) S. G. Telfer, T. M. McLean, M. R. Waterland, *Dalton Trans.* **2011**, *40*, 3097 – 3108.

[18] a) C. S. Johnson, Jr., *Prog. Nucl. Magn. Reson. Spectrosc.* **1999**, *34*, 203 – 256; b) B. Antalek, *Concepts Magn. Reson.* **2002**, *14*, 225 – 258; c) Y. Cohen, L. Avram, L. Frish, *Angew. Chem. Int. Ed.* **2005**, *44*, 520 – 554; *Angew. Chem.* **2005**, *117*, 524 – 560.

[19] M. Scherer, D. L. Caulder, D. W. Johnson, K. N. Raymond, *Angew. Chem. Int. Ed.* **1999**, *38*, 1587 – 1592; *Angew. Chem.* **1999**, *111*, 1689 – 1694.

[20] a) C. Lee, W. Yang, R. G. Parr, *Phys. Rev. B* **1988**, *37*, 785 – 789; b) A. D. Becke, *J. Chem. Phys.* **1993**, *98*, 5648 – 5652; c) M. J. Frisch, et al. Gaussian 09 (Revision D.01); Gaussian, Inc.: Wallingford, CT, **2009**. The full list of authors is provided in the Supporting Information.

[21] We note that while the difference in solvation energies might also affect the difference in binding affinities between thiane and tetrahydropyran, it does not seem to be the primary factor in the current study, since the relation between the binding affinities remains similar in solvents with different polarities (see Table 1).

[22] a) MacroModel, Version 9.7, Schrödinger LLC, New York, **2009**; b) G. J. Kleywegt, VOIDOO, version 3.3.4, Uppsala Software Factory, Uppsala, **2007**.

[23] The Mecozzi–Rebek volume occupancy rule of 55% was originally derived for apolar capsules, and the authors predicted that in case of additional electrostatic polar interactions, a higher occupancy can be expected. Indeed, we have found that for molecular baskets encapsulating heteroalicyclic guests capable of undergoing polar interactions, 63% was the optimal volume occupancy. This is in agreement with the current work: 1,4-Dioxane, with a packing coefficient (PC) of 63%, forms a very stable complex, whereas oxepane with a PC value of 70% is only poorly bound. See: a) S. Mecozzi, J. Rebek, Jr., *Chem. Eur. J.* **1998**, *4*, 1016 – 1022; b) J. Hornung, D. Fankhauser, L. D. Shirtcliff, A. Praetorius, W. B. Schweizer, F. Diederich, *Chem. Eur. J.* **2011**, *17*, 12362 – 12371.

[24] A recent publication describes a flexible tetrahedral capsule, which displays substantial volume variability upon encapsulation of different guests, as well as strong solvent dependence on the binding affinities. See: J. L. Bolliger, T. K. Ronson, M. Ogawa, J. R. Nitschke, *J Am. Chem. Soc.* **2014**, DOI: 10.1021/ja5077102.

[25] a) The U.S. National Toxicology Program, *12th Report on Carcinogens (RoC)*, U.S. Department of Health and Human Services, Washington, D.C. **2011**, pp. 176 – 178; b) U.S. Environmental Protection Agency. *Toxological Review of 1,4-Dioxane*, Washington, DC, **2013**. http://www.epa.gov/iris/toxreviews/0326tr.pdf; c) M. Tahara, T. Obama, Y. Ikarashi, *Int. J. Cosmet. Sci.* **2013**, *35*, 575 – 580.

